

# Virtual and biomolecular screening converge on a selective agonist for GPR30

Cristian G Bologa<sup>1,7</sup>, Chetana M Revankar<sup>2,3,7</sup>, Susan M Young<sup>3</sup>, Bruce S Edwards<sup>3,4</sup>, Jeffrey B Arterburn<sup>5</sup>, Alexander S Kiselyov<sup>6</sup>, Matthew A Parker<sup>6</sup>, Sergey E Tkachenko<sup>6</sup>, Nikolay P Savchuck<sup>6</sup>, Larry A Sklar<sup>3,4</sup>, Tudor I Oprea<sup>1</sup> & Eric R Prossnitz<sup>2,3</sup>

**Estrogen is a hormone critical in the development, normal physiology and pathophysiology<sup>1</sup> of numerous human tissues<sup>2</sup>. The effects of estrogen have traditionally been solely ascribed to estrogen receptor  $\alpha$  (ER $\alpha$ ) and more recently ER $\beta$ , members of the soluble, nuclear ligand-activated family of transcription factors<sup>3</sup>. We have recently shown that the seven-transmembrane G protein-coupled receptor GPR30 binds estrogen with high affinity and resides in the endoplasmic reticulum, where it activates multiple intracellular signaling pathways<sup>4</sup>. To differentiate between the functions of ER $\alpha$  or ER $\beta$  and GPR30, we used a combination of virtual and biomolecular screening to isolate compounds that selectively bind to GPR30. Here we describe the identification of the first GPR30-specific agonist, G-1 (1), capable of activating GPR30 in a complex environment of classical and new estrogen receptors. The development of compounds specific to estrogen receptor family members provides the opportunity to increase our understanding of these receptors and their contribution to estrogen biology.**

With our recent description of an intracellular transmembrane estrogen receptor that initiates multiple signaling pathways<sup>4</sup>, some in common with the traditional estrogen receptors, it is clear that dissecting GPR30-specific cellular and physiological responses is essential to understanding the fundamental mechanisms of estrogen action. To this end, we sought to identify compounds that show highly selective binding to GPR30 as compared with the classical estrogen receptors (ER $\alpha$  and ER $\beta$ ). As GPR30 is known to bind many of the same ligands as classical estrogen receptors (for example, 17 $\beta$ -estradiol (2), 4-hydroxytamoxifen (3), ICI182,780 (4))<sup>4-6</sup>, though with differing cellular effects (for example, ICI182,780 is an ER antagonist but a GPR30 agonist), we screened a library of diverse chemical compounds to identify GPR30-specific ligands.

To minimize the biomolecular screening required, we first used virtual screening<sup>7</sup>, which has recently become increasingly recognized as a complement to bioactivity screening<sup>8</sup>. Virtual screening aims to

sift through vast numbers of structures to rapidly identify those of interest for biological screening. Its experimental counterpart, high-throughput screening, is also aimed at sifting through large numbers of compounds, often based on single-point, single-experiment results. Both procedures rely on the ability to process a large number of structures or compounds<sup>9</sup>. We therefore began by virtually screening a library of 10,000 molecules (preoptimized to be enriched in G protein-coupled receptor (GPCR)-binding ligands based on the concept of the GPCR-privileged substructure<sup>10</sup>) using a combination of 2D- and 3D-similarity approaches. Our combined similarity score attributed 40% weight to 2D fingerprints, 40% to shape-based similarities and 20% to pharmacophore-based similarity. Given this composite score, the top 100 ranked molecules were selected for biomolecular screening.

To accomplish the biomolecular screening, we used a fluorescently labeled estrogen derivative (an Alexa633 conjugate of 17 $\alpha$ -[4-aminomethyl-phenylethynyl]-estra-1,3,5(10)-triene-3,17 $\beta$ -diol (5), E2-Alexa633) that we have recently developed and shown to bind GPR30 as well as ER $\alpha$  and ER $\beta$  (ref. 4). Competitive ligand binding was assessed in transiently transfected COS7 cells, which do not show detectable specific binding of the fluorescent estrogen in the absence of exogenous receptors. Binding was measured with a high-throughput flow cytometric platform (HyperCyt) capable of sampling rates of approximately 1 per s from microplate wells<sup>11,12</sup>. To maximize the bound fluorescent signal, a GPR30-GFP fusion protein was expressed and cells were gated for high levels of green (FL1) fluorescence (that is, GPR30 expression).

Biomolecular screening was carried out with 17 $\beta$ -estradiol as a positive control to block specific binding of E2-Alexa633 to GPR30. Calculation of the Z' factor, a measure of screening assay quality that reflects both assay signal dynamic range and data variation of the signal<sup>13</sup>, yielded a value of 0.5–0.7, indicating the robustness of the assay. From the primary screen performed at a compound concentration of 10  $\mu$ M, three compounds resulted in inhibition of fluorescent estrogen binding greater than 60%. These compounds, as well as numerous intermediate-quality hits, were retested manually from the

<sup>1</sup>Division of Biocomputing, <sup>2</sup>Department of Cell Biology & Physiology, <sup>3</sup>Cancer Research and Treatment Center and <sup>4</sup>Department of Pathology, University of New Mexico Health Sciences Center, Albuquerque, New Mexico 87131, USA. <sup>5</sup>Department of Chemistry and Biochemistry, New Mexico State University, Las Cruces, New Mexico 88003, USA. <sup>6</sup>Chemical Diversity Labs Inc., 11558 Sorrento Valley Road, San Diego, California 92121, USA. <sup>7</sup>These authors contributed equally to this work. Correspondence should be addressed to E.R.P. (EProssnitz@salud.unm.edu) or T.I.O. (TOprea@salud.unm.edu).

Received 23 December 2005; accepted 9 February 2006; published online 05 March 2006; doi:10.1038/nchembio775

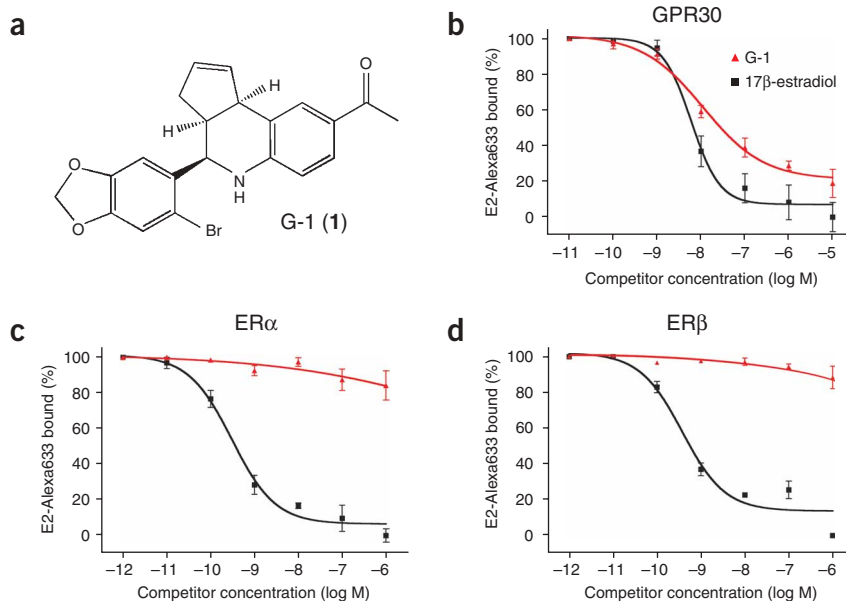


**Figure 1** Structure and ligand-binding properties of G-1. (a) Chemical structure of compound G-1. (b–d) Ligand-binding affinities of 17β-estradiol and G-1 for GPR30, ERα and ERβ. Results of competitive ligand-binding assays using 2 nM E2-Alexa633 and the indicated concentration of either 17β-estradiol (■) or G-1 (▲) in COS7 cells transfected with either GPR30-GFP (b), ERα-GFP (c) or ERβ-GFP (d). Data indicate the mean ± s.e.m. of three separate experiments.

Hill coefficient was 0.6, suggesting that there could be two binding sites of similar but not identical affinity. These results indicate that G-1 has not only very high affinity for GPR30 but also great selectivity toward GPR30 as compared with ERα and ERβ.

We next examined the functional capabilities of G-1 versus estrogen with respect to the rapid mobilization of intracellular calcium. Whereas 17β-estradiol initiates a very rapid ( $t_{1/2} < 2$  s) rise in intracellular calcium concentrations, G-1 produces a slower ( $t_{1/2} \sim 30$  s) but ultimately comparable calcium increase (Fig. 2a). The specificity of the response is shown by the fact that neither 17β-estradiol nor G-1 has an effect on control COS7 cells (not expressing GPR30) and that 17α-estradiol (6) has no effect on GPR30-expressing COS7 cells. To confirm the selectivity of G-1 toward GPR30 as compared with ERα and ERβ (as suggested by the binding assays), we also examined calcium mobilization in COS7 cells expressing either ERα or ERβ. In neither case did G-1 elicit a calcium response (Fig. 2b,c). This is in contrast to 17β-estradiol, which yields a rapid response with both ERα and ERβ. As observed with GPR30, 17α-estradiol had no effect on ERα or ERβ. Dose-response determinations showed that the mobilization of intracellular calcium initiated by G-1 in the presence of GPR30 was concentration dependent, with a half-maximal effector concentration ( $EC_{50}$ ) of about 2 nM (Fig. 2d,e), similar to the binding affinity of G-1 for GPR30, compared with an  $EC_{50}$  for 17β-estradiol of approximately 0.3 nM. In addition to calcium mobilization, we have shown that stimulation of ERα, ERβ and GPR30 with estrogen results in phosphatidylinositol 3-kinase (PI3K) activation, resulting in the nuclear

master plate for their ability to inhibit binding of fluorescent estrogen to GPR30; this revealed that only compound 92, a substituted dihydroquinoline (Fig. 1a), consistently inhibited binding. This compound will be referred to henceforth as G-1 (GPR30-specific compound 1). Its structure, which was subsequently reconfirmed by LC-MS and  $^1\text{H-NMR}$ , is racemic but diastomerically pure (see Methods).

To characterize the binding properties of G-1 in greater depth, we determined the binding affinity to GPR30 and the binding specificity with respect to ERα and ERβ. Competition binding of the fluorescent estrogen by 17β-estradiol in GPR30-expressing cells yielded a  $K_i$  of 5.7 nM (similar to the value of 6.6 nM we reported previously), whereas the  $K_i$  for G-1 was 11 nM (Fig. 1b). Competition binding in ERα- and ERβ-expressing cells yielded  $K_i$  values for 17β-estradiol of 0.30 and 0.38 nM, respectively, with no substantial binding of G-1 at concentrations up to 1 μM (Fig. 1c,d). The Hill coefficients for the estrogen-competition binding curves were approximately 1.0 (1.2, 0.9 and 0.9 for GPR30, ERα and ERβ, respectively), whereas for G-1, the

calcium increase (Fig. 2a). The specificity of the response is shown by the fact that neither 17β-estradiol nor G-1 has an effect on control COS7 cells (not expressing GPR30) and that 17α-estradiol (6) has no effect on GPR30-expressing COS7 cells. To confirm the selectivity of G-1 toward GPR30 as compared with ERα and ERβ (as suggested by the binding assays), we also examined calcium mobilization in COS7 cells expressing either ERα or ERβ. In neither case did G-1 elicit a calcium response (Fig. 2b,c). This is in contrast to 17β-estradiol, which yields a rapid response with both ERα and ERβ. As observed with GPR30, 17α-estradiol had no effect on ERα or ERβ. Dose-response determinations showed that the mobilization of intracellular calcium initiated by G-1 in the presence of GPR30 was concentration dependent, with a half-maximal effector concentration ( $EC_{50}$ ) of about 2 nM (Fig. 2d,e), similar to the binding affinity of G-1 for GPR30, compared with an  $EC_{50}$  for 17β-estradiol of approximately 0.3 nM. In addition to calcium mobilization, we have shown that stimulation of ERα, ERβ and GPR30 with estrogen results in phosphatidylinositol 3-kinase (PI3K) activation, resulting in the nuclear

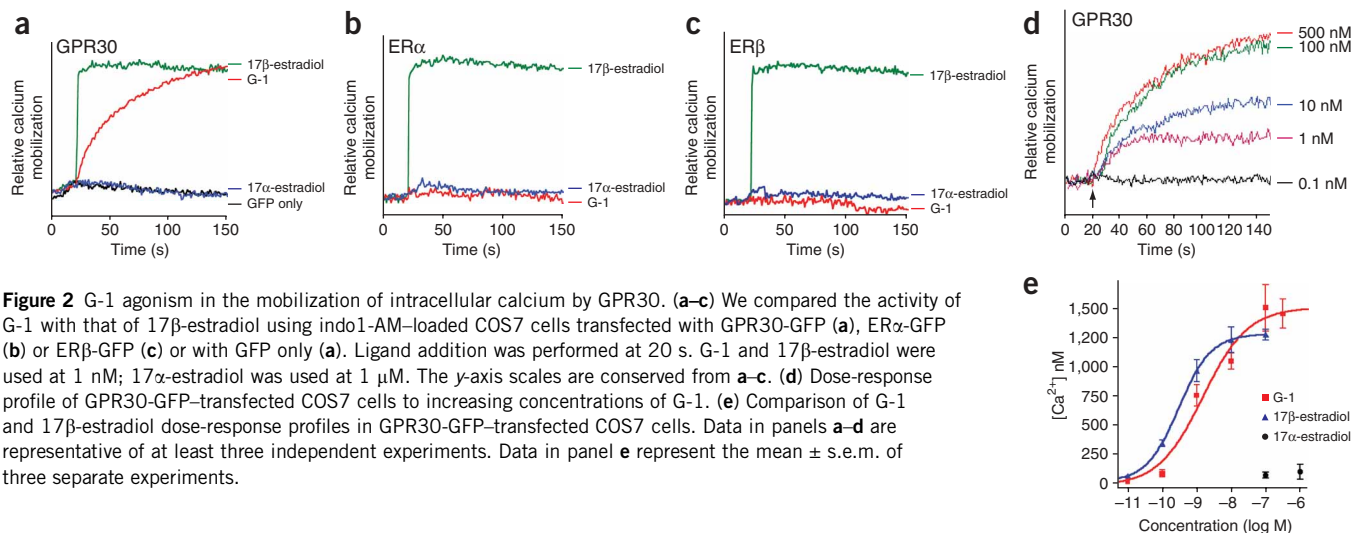


**Figure 2** G-1 agonism in the mobilization of intracellular calcium by GPR30. (a–c) We compared the activity of G-1 with that of 17β-estradiol using indo1-AM-loaded COS7 cells transfected with GPR30-GFP (a), ERα-GFP (b) or ERβ-GFP (c) or with GFP only (a). Ligand addition was performed at 20 s. G-1 and 17β-estradiol were used at 1 nM; 17α-estradiol was used at 1 μM. The y-axis scales are conserved from a–c. (d) Dose-response profile of GPR30-GFP-transfected COS7 cells to increasing concentrations of G-1. (e) Comparison of G-1 and 17β-estradiol dose-response profiles in GPR30-GFP-transfected COS7 cells. Data in panels a–d are representative of at least three independent experiments. Data in panel e represent the mean ± s.e.m. of three separate experiments.

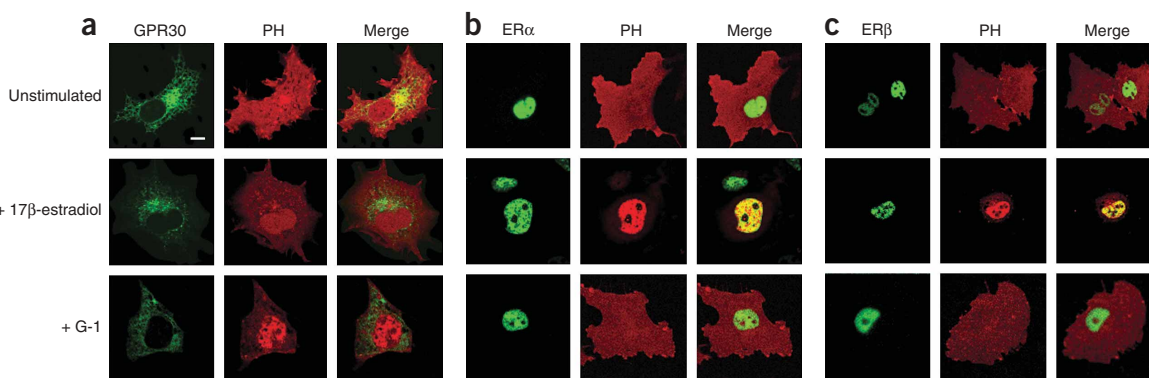


**Figure 3** G-1 agonism in PI3K activation by GPR30. We compared the activity of G-1 with that of 17 $\beta$ -estradiol using COS7 cells transfected with Akt-PH-mRFP1 and either GPR30-GFP (a), ER $\alpha$ -GFP (b) or ER $\beta$ -GFP (c). 17 $\beta$ -estradiol and G-1 were used at 1 nM and 10 nM, respectively. The white bar in upper left panel of a denotes 10  $\mu$ m. Data are representative of three independent experiments.

accumulation of phosphatidylinositol 3,4,5-triphosphate (PIP3) (ref. 4). This is shown by the translocation of a reporter, the pleckstrin homology (PH) domain of Akt fused to a fluorescent protein, in response to the *de novo* production of PIP3 by PI3K (ref. 14). To confirm our hypothesis that G-1 activates a similar complement of signaling pathways as estrogen, we examined the activation of PI3K in receptor-transfected COS7 cells. As previously observed, estrogen stimulates the nuclear accumulation of PIP3 through all three receptors. However, as observed for calcium signaling, G-1 selectively activated GPR30 and not ER $\alpha$  or ER $\beta$  (Fig. 3). In total, these results indicate that G-1 binds and activates GPR30 with great specificity over both ER types.

These results suggest that we should be able to selectively target GPR30 as opposed to ERs in cells that express both receptors. To test this, we cotransfected cells with GPR30—monomeric red fluorescent protein-1 (GFP30-mRFP1) and ER $\alpha$ -GFP, which localize to distinct subcellular compartments (the nucleus and endoplasmic reticulum, respectively). The receptors were visualized with E2-Alexa633, and cells were incubated in the presence or absence of G-1 (Fig. 4a). In the

absence of competitor, fluorescent estrogen staining was seen throughout the cell (nucleus and endoplasmic reticulum), representing the sum of the individual compartments. Competition with 17 $\beta$ -estradiol blocked binding of the E2-Alexa633 to both ER $\alpha$  and GPR30. However, in the presence of G-1, staining in the endoplasmic reticulum was selectively lost over that in the nucleus (for both ER $\alpha$  and ER $\beta$ ). This showed that in the same cell, G-1 selectively binds GPR30 and not ERs.

Next, we sought to determine whether G-1 activates endogenously expressed GPR30. We have previously shown that estrogen-mediated activation of PI3K in SKBr3 breast cancer cells, which are ER $\alpha$  and ER $\beta$  negative, occurs exclusively through GPR30. We therefore tested whether G-1 was able to activate PI3K in SKBr3 cells. We found that G-1, like estrogen, activated PI3K, resulting in the nuclear accumulation of PIP3 in both SKBr3 cells (that express only GPR30) as well as in MCF7 cells (which express both GPR30 and classical ERs, with high levels of ER $\alpha$  and low levels of ER $\beta$ ) (Fig. 4b). This latter result in MCF7 cells suggests that the estrogen-mediated response is occurring at least in part through GPR30. To investigate the physiological

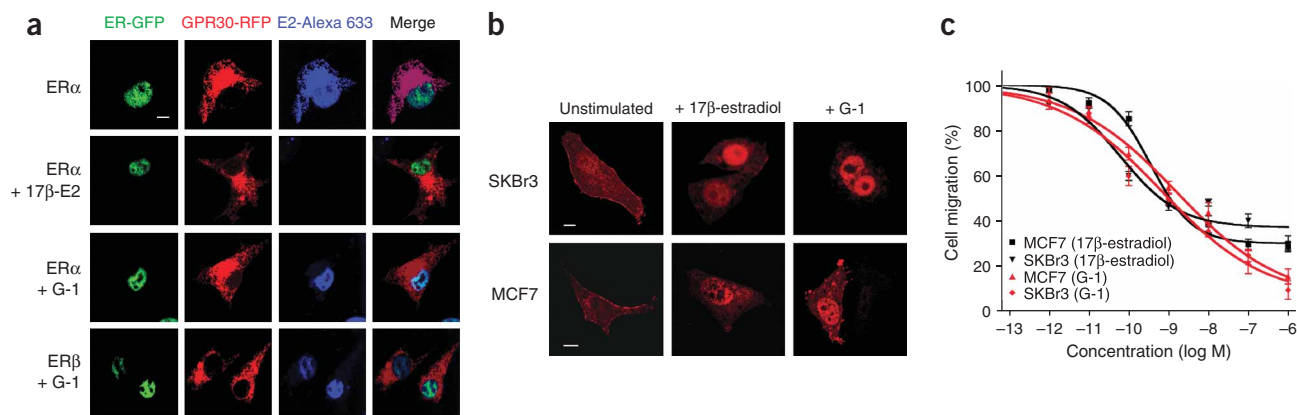


**Figure 4** Selective targeting of GPR30 versus ER $\alpha$  or ER $\beta$  by G-1. (a) COS7 cells cotransfected with either GPR30-mRFP1 and ER $\alpha$ -GFP or GPR30-mRFP1 and ER $\beta$ -GFP as indicated and stained with E2-Alexa633 in the absence or presence of excess 17 $\beta$ -estradiol or G-1 (1  $\mu$ M). Although excess 17 $\beta$ -estradiol prevents binding of E2-Alexa633 to both ER and GPR30, G-1 selectively competes for binding to GPR30 in cells that also express ERs. (b) SKBr3 breast cancer cells, which endogenously express only GPR30, and MCF7 cells, which express GPR30 and ER $\alpha$ / $\beta$ , after transfection with Akt-PH-mRFP1 and stimulation with either 1 nM 17 $\beta$ -estradiol or 10 nM G-1. White bars denote 10  $\mu$ m. (c) Cell migration of SKBr3 and MCF7 cells through a Transwell chamber in response to chemoattractant. Cells in the upper chamber were treated with either 17 $\beta$ -estradiol or G-1 as indicated. Data are representative of three independent experiments or represent the mean  $\pm$  s.e.m. of three separate experiments with all *P* values < 0.05.

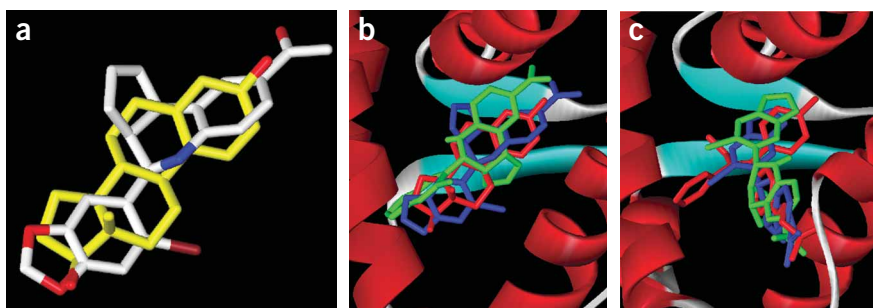


**Figure 5** G-1 and 17 $\beta$ -estradiol structural overlap and docking to ER $\alpha$ . (a) Overlay of stick-model representations of G-1 and 17 $\beta$ -estradiol to maximize spatial overlap by the shape-matching procedure of ROCS. 17 $\beta$ -estradiol is shown in yellow, G-1 in light gray, oxygen atoms in bright red, nitrogen in blue and bromine in dark red. (b,c) Docking of G-1 into the 17 $\beta$ -estradiol- (b) and 4-hydroxytamoxifen-bound (c) conformations of ER $\alpha$  (1ERE and 3ERT, respectively). The endogenous ligand (17 $\beta$ -estradiol in b and 4-hydroxytamoxifen in c) as found in each crystal structure is shown in red. The optimal shape overlays of G-1 onto 17 $\beta$ -estradiol (as shown in a) and 4-hydroxytamoxifen are shown in blue. The optimally ER $\alpha$ -docked structures of G-1 based on protein interactions as computed using AutoDock are shown in green.

function of GPR30 using G-1, we examined cell migration in response to estrogen and G-1 (Fig. 4c). Using a Transwell migration apparatus (Costar), we demonstrated that in response to chemoattractant (serum, EGF and insulin), both estrogen, as previously documented<sup>15</sup>, and G-1 inhibited migration of SKBr3 cells (with half-maximal inhibitory concentration (IC<sub>50</sub>) values for estrogen and G-1 of 0.1 and 0.7 nM, respectively) and MCF7 cells (with IC<sub>50</sub> values for estrogen and G-1 of 0.4 and 1.6 nM, respectively). The four- to seven-fold greater activity of estrogen as compared with G-1 is consistent with the relative differences between the two compounds in both binding affinity (Fig. 1) and signaling capacity (Fig. 2e). Overall, these results confirm that G-1 can selectively bind GPR30 in the same cell where ERs are present and furthermore that G-1 can activate endogenously expressed GPR30, resulting in physiologic responses even in cells expressing multiple estrogen receptor types.

In summary, we have identified a nonsteroidal, high-affinity, highly selective agonist of GPR30. This represents the first description of a compound that can distinguish between GPR30 and the classical estrogen receptors. Superimposition of the structure of 17 $\beta$ -estradiol with G-1 using rapid overlay of chemical structures (ROCS)<sup>16</sup> reveals a high degree of shape similarity between both enantiomers of G-1 and 17 $\beta$ -estradiol (Fig. 5a). To examine why G-1 shows such high selectivity for GPR30 over ERs, we performed docking experiments (with AutoDock (<http://www.scripps.edu/mb/olson/doc/autodock/>)) of both enantiomers of G-1 (the structure shown in Fig. 1a as well as its enantiomer) into the ligand-binding pocket of ER $\alpha$  in both its 17 $\beta$ -estradiol- and 4-hydroxytamoxifen-bound crystallographic conformations (see Methods for Protein Data Bank accession codes). To obtain a computational estimate of the binding affinity, both native ligands were docked into their respective structures as well. Full flexibility for the ligands was assumed, and no initial positioning of the ligand into the binding site was performed. The results of the docking experiment for the enantiomer from Figure 1a are shown in Figure 5b,c, and the computationally predicted binding affinities for both enantiomers are summarized in Supplementary Table 1. When docked into the agonist-bound conformation of ER $\alpha$  (Fig. 5b), both enantiomers of G-1 are estimated to have an affinity approximately three orders of magnitude worse than that of 17 $\beta$ -estradiol<sup>17</sup>. For example, in the best-docked poses, both G-1 enantiomers do not

present the hydrogen-bonding pattern of 17 $\beta$ -estradiol (that is, no interaction with Glu353 and His524), and moreover they show steric clashes with multiple backbone atoms. The estimated  $K_i$  values from Supplementary Table 1 appear to suggest that G-1 might bind ER $\alpha$  as a low-affinity antagonist. When docked into the 4-hydroxytamoxifen-bound conformation of ER $\alpha$  (Fig. 5c), both G-1 enantiomers are estimated to have affinities approximately two orders of magnitude above that of 4-hydroxytamoxifen. Once again, however, both enantiomers of G-1 fail to interact with key hydrogen bond partners, while showing steric clashes with the receptor ligand-binding site. Thus, we conclude that G-1 cannot be positioned to interact optimally with either the agonist- or antagonist-occupied conformations of ER $\alpha$ , a finding consistent with our experimental results.

In conclusion, the overall discovery process was facilitated by the preliminary step of virtual or *in silico* screening combined with technological advances, including the use of a new fluorescent estrogen derivative in the binding assay, a high-throughput flow cytometric platform (HyperCyt) and new assays of estrogen-mediated PI3K activation. The discovery of the first GPR30-specific agonist that does not bind classical ERs should facilitate further physiological experiments to define the role of GPR30 *in vivo* and open the door to the generation of diagnostics and therapeutics directed at individual estrogen receptors.

## METHODS

**Database processing.** A database of 10,000 in-house molecules (CDLDB) provided by Chemical Diversity Labs, to which 17 $\beta$ -estradiol was added, was processed according to a procedure detailed elsewhere<sup>18</sup>. Very briefly, canonical isomeric SMILES (ref. 19, Daylight Toolkit v4.81, Daylight Chemical Information Systems) were derived from input structures. Smi2fp\_ascii (Daylight Chemical Information Systems) and MACCSKeys320 Generator (Mesa Analytics and Computing) software was used to compute Daylight and MDL<sup>20</sup> fingerprints, respectively, and 3D structures were derived with the OMEGA software from OpenEye Scientific Software.

**2D-based similarity.** Using 17 $\beta$ -estradiol as a reference point, we computed similarity coefficients using both Daylight and MDL fingerprints for CDLDB using Tanimoto's symmetric distance-between-patterns<sup>21</sup> and Tversky's asymmetric contrast model<sup>22</sup>. Tanimoto similarities are symmetric (that is, when molecule A is compared to molecule B and vice versa, the Tanimoto coefficients are identical), whereas Tversky similarity is asymmetric (that is, the two coefficient values differ). In total, six 2D-based similarity coefficients were obtained.

**3D-based similarity.** Using the 3D structure of 17 $\beta$ -estradiol as a reference point, we obtained shape-similarity coefficients using the Tanimoto<sup>21</sup> and Tversky<sup>22</sup> formulas using ROCS, rapid overlay of chemical structures<sup>16</sup>, a Gaussian-shape-volume-overlap filter that identifies shapes that match the query molecule. Another similarity metric, using Euclidian distances in a nine-dimensional principal component analysis (PCA) space<sup>23</sup>, was derived from ALMOND descriptors<sup>24</sup>. ALMOND encodes hydrophobic, H-bond donor and H-bond acceptor pharmacophoric elements derived from molecular interaction fields computed with GRID<sup>25</sup> into a reduced set of variables.

**Final similarity score.** Our combined similarity score attributed 40% weight to 2D fingerprints, 40% to the shape-based similarities and 20% to pharmacophore-based similarity. Thus, Tanimoto and Tversky (substructure and

superstructure) coefficients were given a 6.66% contribution each, for both Daylight and MDL fingerprints, and a 13.33% contribution each for shape. The Euclidian distance in PCA was given a 20% weight to the final score. Given this composite score, the top 100 ranked molecules were selected for physical screening.

**Ligand overlaying and docking.** To overlay the structure of G-1 and 17 $\beta$ -estradiol or 4-hydroxytamoxifen, we used the shape-matching procedure of ROCS with full conformational flexibility and the receptor-bound conformations of 17 $\beta$ -estradiol and 4-hydroxytamoxifen. We performed docking of ligands into ER $\alpha$  using AutoDock 3.0.5 (ref. 26). We selected the 17 $\beta$ -estradiol co-crystallized with ER $\alpha$  in its agonist-bound conformation and 4-hydroxytamoxifen co-crystallized with ER $\alpha$  in its antagonist-bound conformation. The structure of G-1 was docked in the ligand-binding site of the two conformations of ER $\alpha$ , after extracting 17 $\beta$ -estradiol and 4-hydroxytamoxifen, respectively. To get a computational estimate of the binding affinity, both native ligands were docked into their respective receptors as well. We assumed full ligand flexibility, and no initial positioning of the ligand into the binding pocket was performed.

**Ligand-binding assays.** We performed binding assays as described<sup>4</sup>. Briefly, COS7 cells were transiently transfected with either nuclear estrogen receptor (ER $\alpha$ -GFP or ER $\beta$ -GFP) or GPR30-GFP and serum starved for 24 h before assay. For HyperCyt screening, cells ( $\sim 5 \times 10^4$ ) were incubated with 10  $\mu$ M compound for 20 min in a final volume of 10  $\mu$ l before addition of 10  $\mu$ l 8 nM E2-Alexa633 diluted in saponin-based permeabilization buffer. Following 10 min at 37  $^{\circ}$ C, cells were washed once with 200  $\mu$ l PBS in 1% BSA, and 2- $\mu$ l samples were analyzed on a FACS Calibur. Cell Quest time bin-based data produced by the HyperCyt system were analyzed with IDLQuery software as described<sup>27</sup>. We analyzed dose responses manually using the indicated concentration of competitor and 2 nM E2-Alexa633. Nonspecific binding was determined in presence of 100 nM 17 $\beta$ -estradiol. We carried out labeling of cells for microscopy as previously described<sup>4</sup> using 1  $\mu$ M 17 $\beta$ -estradiol or G-1 to determine nonspecific binding. Competition binding studies were analyzed with Prism 4.0 (GraphPad).

**Intracellular calcium mobilization.** Transfected COS7 cells ( $5 \times 10^6$ ) were incubated in HBSS containing 5  $\mu$ M Indo1-AM and 0.05% pluronic acid for 30 min at 25  $^{\circ}$ C. Cells were then washed once with HBSS and resuspended in HBSS at a density of  $10^7$  cells per ml. We determined Ca<sup>2+</sup> mobilization ratiometrically using  $\lambda_{ex}$  340 nm and  $\lambda_{em}$  400/490 nm at 37  $^{\circ}$ C in a spectrofluorometer (QM-2000-2, Photon Technology International) equipped with a magnetic stirrer. The relative 490/400 nm ratio was plotted as a function of time.

**PI3K activation.** We used the PIP3 binding domain of Akt fused to mRFP1 (PH-mRFP1) to assess PIP3 production by PI3K. COS7 cells cotransfected with GPR30-GFP or ER $\alpha$ -GFP and PH-mRFP1 were plated on coverslips and serum starved for 24 h, and then they were stimulated with ligands as indicated. The cells on coverslips were fixed with 2% PFA in PBS, washed and mounted in Vectashield (Vector Labs). The cells were analyzed by confocal microscopy with a Zeiss LSM510.

**Cell migration.** Migration assays were carried out with 6.5 mm Transwells with an 8- $\mu$ m pore size (Costar Corning) as previously described<sup>28</sup>. The undersurface of the Transwell was coated overnight at 4  $^{\circ}$ C with approximately 50  $\mu$ g ml<sup>-1</sup> rat-tail collagen and washed with PBS. DMEM/F12 (600  $\mu$ l) supplemented with 10% FBS, 10 ng ml<sup>-1</sup> of EGF and 10  $\mu$ g ml<sup>-1</sup> of insulin was added to the lower chamber as chemoattractant. SKBr3 or MCF7 cells (75,000 cells) in serum-free DMEM/F12 (150  $\mu$ l) were treated with ethanol (control), 17 $\beta$ -estradiol or G-1 for 15 min at 37  $^{\circ}$ C before loading in the upper chamber. After incubation for 48 h at 37  $^{\circ}$ C, the remaining cells were wiped from the upper surface of the membrane with a damp cotton swab. The migrated cells on the undersurface of the membrane were fixed with 2% paraformaldehyde and stained with 1% crystal violet. Quantification of cells was performed by counting the number of cells per field in five random fields per membrane, and migration was calculated as: % migration = (number of cells in treated/number of cells in ethanol control)  $\times$  100.

**Chemical synthesis and characterization of G-1.** The compound G-1 (1-[4-(6-bromobenzo[1,3]dioxol-5-yl)-3a,4,5,9b-tetrahydro-3H-cyclopenta[c]quinolin-8-yl]-ethanone) was synthesized through a previously described method<sup>29</sup>: trifluoroacetic acid (1.52 g, 13.3 mmol) was added dropwise to a solution of 4-aminoacetophenone (7) (2.0 g, 14.8 mmol) in acetonitrile. Freshly distilled cyclopentadiene (8) (3.91 g, 59.2 mmol) was added, followed by 6-bromopiperonal (9) (3.39 g, 14.8 mmol). The mixture was stirred overnight at 25  $^{\circ}$ C, and the product was isolated from an aliquot of the mixture by preparative HPLC (C<sub>18</sub>, 5–95% CH<sub>3</sub>CN in H<sub>2</sub>O gradient, 0.05% trifluoroacetic acid), with a yield of approximately 70%.

Spectroscopic characterization of G-1 yielded the following: <sup>1</sup>H NMR (400 MHz, DMSO-d<sub>6</sub>):  $\delta$  7.62 (s, 1H), 7.53 (dd, 1H, J = 1.9 Hz, 8.6 Hz), 7.26 (s, 1H), 7.11 (s, 1H), 6.73 (d, 1H, J = 8.4 Hz), 6.47 (s, 1H), 6.09 (d, 2H, J = 9.1 Hz), 5.97 (m, 1H), 5.60 (broad d, 1H, J = 5.7 Hz), 4.78 (d, 1H, J = 3.3 Hz), 4.05 (d, 1H, J = 8.8 Hz), 3.02 (q, 1H, J = 8.4 Hz), 2.41 (s, 3H), 2.36–2.44 (m, 1H), 1.66 (broad dd, 1H, J = 7–9 Hz). <sup>13</sup>C NMR (100 MHz, CD<sub>3</sub>CN):  $\delta$  25.76, 31.61, 42.33, 45.50, 56.15, 102.69, 108.44, 112.75, 112.84, 115.49, 124.93, 127.57, 128.48, 130.31, 130.33, 134.19, 134.64, 147.95, 148.04, 150.94, 196.33. HRMS (*m/z*): calcd. C<sub>21</sub>H<sub>18</sub>BrNO<sub>3</sub> requires MH<sup>+</sup>, 412.0543; found MH<sup>+</sup>, 412.0539.

G-1 was analyzed by standard LC-MS methods with positive ion detection. The LC-MS chromatogram showed the correct molecular (MH<sup>+</sup>) ion as well as a single peak by both UV (254 nm) and ELSD detection. Only one diastereomer was obtained; examination of the <sup>1</sup>H NMR data shows H-4 (4.78 p.p.m.) with a coupling constant of 3.3 Hz, indicating a *cis* orientation of the cyclopentene ring and phenyl group, in agreement with the all-*cis* stereochemistry determined by other groups for similar imino Diels-Alder reactions using cyclopentadiene<sup>30</sup>. Thus G-1 is a racemic but diastereomerically pure compound.

**Accession codes.** Protein Data Bank: 17 $\beta$ -estradiol-bound conformation of ER $\alpha$ , 1ERE; 4-hydroxytamoxifen-bound conformation of ER $\alpha$ , 3ERT.

*Note: Supplementary information is available on the Nature Chemical Biology website.*

#### ACKNOWLEDGMENTS

This work was supported by US National Institutes of Health (NIH) grant AI36357 and a University of New Mexico Cancer Research and Treatment Center Translational Research Grant to E.R.P., by NIH grant EB00264 to L.A.S., and by support from the New Mexico Tobacco Settlement fund to C.G.B. and T.I.O. Additional support was provided by the New Mexico Cancer Research and Treatment Center (CRTC; NIH 1. P30 CA118100), the New Mexico Molecular Libraries Screening Center (NIH MH074425) and the New Mexico Center for Environmental Health Sciences (NIH ES012072). Flow cytometry data and confocal images in this study were generated in the Flow Cytometry and Fluorescence Microscopy Facilities, respectively, at the University of New Mexico Health Sciences Center, which received support from National Center for Research Resources (NCRR) 1 S10 RR14668, National Science Foundation MCB9982161, NCRR P20 RR11830, National Cancer Institute R24 CA88339, NCRR S10 RR19287, NCRR S10 RR016918, the University of New Mexico Health Sciences Center, and the University of New Mexico CRTC.

#### COMPETING INTERESTS STATEMENT

The authors declare that they have no competing financial interests.

Published online at <http://www.nature.com/naturechemicalbiology/>  
Reprints and permissions information is available online at <http://npg.nature.com/reprintsandpermissions/>

- Osborne, C.K. & Schiff, R. Estrogen-receptor biology: continuing progress and therapeutic implications. *J. Clin. Oncol.* **23**, 1616–1622 (2005).
- Hall, J.M., Couse, J.F. & Korach, K.S. The multifaceted mechanisms of estradiol and estrogen receptor signaling. *J. Biol. Chem.* **276**, 36869–36872 (2001).
- Korach, K.S. *et al.* Update on animal models developed for analyses of estrogen receptor biological activity. *J. Steroid Biochem. Mol. Biol.* **86**, 387–391 (2003).
- Revankar, C.M., Cimino, D.F., Sklar, L.A., Arterburn, J.B. & Prossnitz, E.R. A transmembrane intracellular estrogen receptor mediates rapid cell signaling. *Science* **307**, 1625–1630 (2005).
- Thomas, P., Pang, Y., Filardo, E.J. & Dong, J. Identity of an estrogen membrane receptor coupled to a G-protein in human breast cancer cells. *Endocrinology* **146**, 624–632 (2005).

- Filardo, E.J., Quinn, J.A., Bland, K.I. & Frackelton, A.R., Jr. Estrogen-induced activation of Erk-1 and Erk-2 requires the G protein-coupled receptor homolog, GPR30, and occurs via trans-activation of the epidermal growth factor receptor through release of HB-EGF. *Mol. Endocrinol.* **14**, 1649–1660 (2000).
- Walters, W.P., Stahl, M.T. & Murcko, M.A. Virtual screening—an overview. *Drug Discov. Today* **3**, 160–178 (1998).
- Oprea, T.I. & Matter, H. Integrating virtual screening in lead discovery. *Curr. Opin. Chem. Biol.* **8**, 349–358 (2004).
- Oprea, T.I., Li, J., Muresan, S. & Mattes, K.C. High throughput and virtual screening: choosing the appropriate leads, in EuroQSAR 2002. In *Designing Drugs and Crop Protectants: Processes, Problems and Solutions* (eds. Ford, M., Livingstone, D., Dearden, J. and Van de Waterbeemd, H.) (Blackwell Publishing, New York, 2003).
- Savchuk, N.P., Tkachenko, S.E. & Balakin, K.V. Rational design of GPCR-specific combinatorial libraries based on the concept of privileged substructures. in *Cheminformatics in Drug Discovery* (ed. Oprea, T.I.) 287–313 (Wiley VCH, Weinheim, 2005).
- Edwards, B.S., Oprea, T., Prossnitz, E.R. & Sklar, L.A. Flow cytometry for high-throughput, high-content screening. *Curr. Opin. Chem. Biol.* **8**, 392–398 (2004).
- Waller, A. *et al.* Techniques: GPCR assembly, pharmacology and screening by flow cytometry. *Trends Pharmacol. Sci.* **25**, 663–669 (2004).
- Zhang, J.H., Chung, T.D. & Oldenburg, K.R. A simple statistical parameter for use in evaluation and validation of high throughput screening assays. *J. Biomol. Screen.* **4**, 67–73 (1999).
- Balla, T. & Varnai, P. Visualizing cellular phosphoinositide pools with GFP-fused protein-modules. *Sci. STKE* **2002**, PL3 (2002).
- Rochefort, H. *et al.* Estrogen receptor mediated inhibition of cancer cell invasion and motility: an overview. *J. Steroid Biochem. Mol. Biol.* **65**, 163–168 (1998).
- Grant, J.A., Pickup, B.T. & Nicholls, A. A smooth permittivity function for Poisson-Boltzmann solvation methods. *J. Comput. Chem.* **22**, 608–640 (2001).
- Rich, R.L. *et al.* Kinetic analysis of estrogen receptor/ligand interactions. *Proc. Natl. Acad. Sci. USA* **99**, 8562–8567 (2002).
- Olah, M., Bologa, C.G. & Oprea, T.I. Strategies for compound selection. *Curr. Drug Discov. Technol.* **1**, 211–220 (2004).
- Weininger, D. SMILES, a chemical language and information system. 1. Introduction to methodology and encoding rules. *J. Chem. Inf. Comput. Sci.* **28**, 31–36 (1988).
- Durant, J.L., Leland, B.A., Henry, D.R. & Nourse, J.G. Reoptimization of MDL keys for use in drug discovery. *J. Chem. Inf. Comput. Sci.* **42**, 1273–1280 (2002).
- Tanimoto, T.T. Non-linear model for a computer assisted medical diagnostic procedure. *Trans. NY Acad. Sci.* **23**, 576–580 (1961).
- Tversky, A. Features of similarity. *Psychol. Rev.* **84**, 327–352 (1977).
- Jackson, J.E. *A Users Guide to Principal Components* (Wiley-VCH, New York, 1991).
- Pastor, M., Cruciani, G., McLay, I., Pickett, S. & Clementi, S. GRIND-INdependent descriptors (GRIND): a novel class of alignment-independent three-dimensional molecular descriptors. *J. Med. Chem.* **43**, 3233–3243 (2000).
- Goodford, P.J. A computational procedure for determining energetically favorable binding sites on biologically important macromolecules. *J. Med. Chem.* **28**, 849–857 (1985).
- Morris, G.M. *et al.* Automated docking using a Lamarckian genetic algorithm and empirical binding free energy function. *J. Comp. Chem.* **19**, 1639–1662 (1998).
- Ramirez, S., Aiken, C.T., Andrzejewski, B., Sklar, L.A. & Edwards, B.S. High-throughput flow cytometry: validation in microvolume bioassays. *Cytometry A* **53**, 55–65 (2003).
- Deryugina, E.I. *et al.* MT1-MMP initiates activation of pro-MMP-2 and integrin alphavbeta3 promotes maturation of MMP-2 in breast carcinoma cells. *Exp. Cell Res.* **263**, 209–223 (2001).
- Baudelle, R., Melnyk, P., Deprez, B. & Tartar, A. Parallel synthesis of polysubstituted tetrahydroquinolines. *Tetrahedron* **54**, 4125–4140 (1998).
- Sartori, G., Bigi, F., Maggi, R., Mazzacani, A. & Oppici, G. Clay/water mixtures—a heterogeneous and ecologically efficient catalyst for the three-component stereoselective synthesis of tetrahydroquinolines. *Eur. J. Org. Chem.* **2001**, 2513–2518 (2001).